

Neutralino Search

Simulations

with G Jungman

Steady state: $N_{exp} = N_{in}$

Backward-in-time approach

Generate X_0

Propagate to infinity $X_0 \rightarrow X_\infty$

Given $P(X_\infty)$ find weight $w(X_0)$

Main approximations

Sun:

Stationary protons

constant density

No planets

No "direct" annihilations

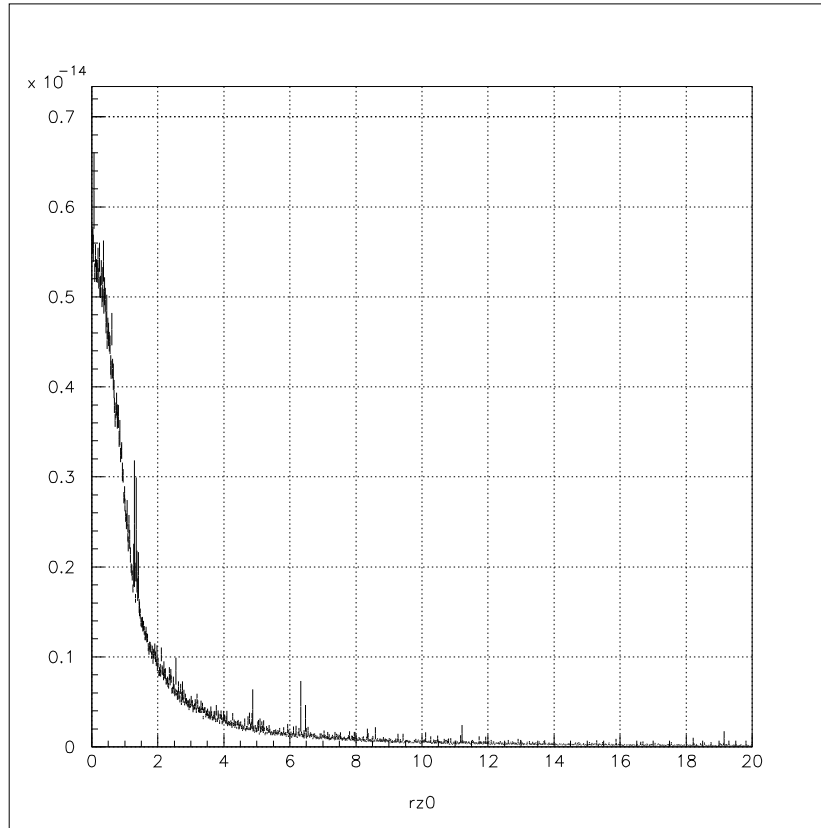


Figure 2: Radial distribution of the annihilation points for $m_\chi = 200$ (GeV) and $\sigma_{p\chi} = 10^{-43}$ (cm^2). Vertical scale is arbitrary, horizontal is in R_\odot , more than $25 \cdot 10^6$ simulated particles.

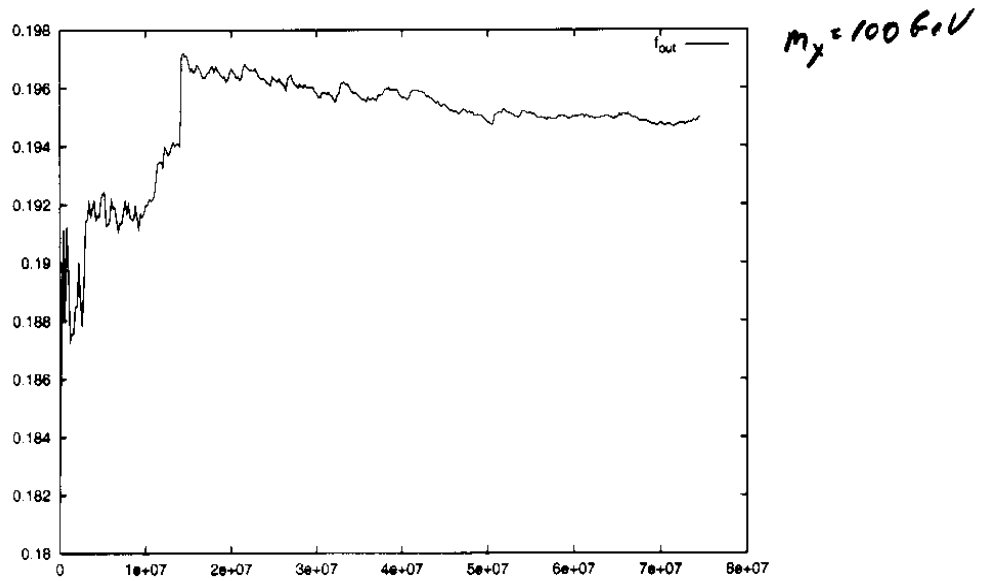


Figure 4: Fraction between R_{\odot} and $2R_{\odot}$ as a function of number of particles in calculation.

Per kebs/s

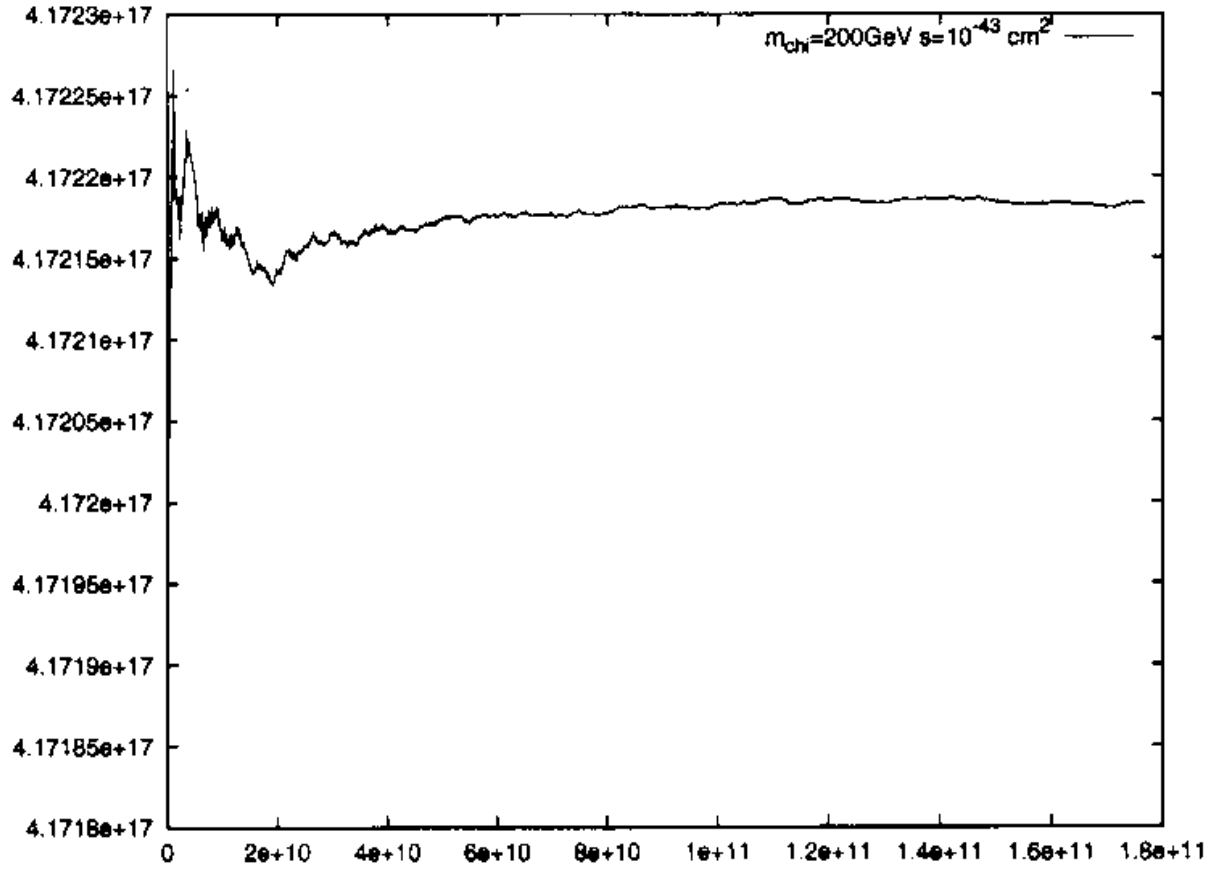


Figure 3: Capture rate (integral) as a function of number of particles in calculation

$m_\chi, (TeV)$	f_{out}	$I(m_\chi) \times \frac{\sigma_{\chi\chi}}{10^{-43}cm^2} \frac{\rho_0}{0.3GeV/cm^3}, (s^{-1})$
0.1	0.195	$1.65 \cdot 10^{18}$
0.2	0.196	$4.17 \cdot 10^{17}$
0.5	0.2	$6.72 \cdot 10^{16}$
1.0	0.199	$1.68 \cdot 10^{16}$
2.0	0.201	$4.22 \cdot 10^{15}$
5.0	0.2	$6.72 \cdot 10^{14}$
10.0	0.2	$1.69 \cdot 10^{14}$
20.0		$4.22 \cdot 10^{13}$
50.0		$6.75 \cdot 10^{12}$

Table 4: Simulation/computation results

Predicted photon flux
 due to neutrino annihilations

$$\frac{dF}{dE} = \rho_0 \sigma_{py} b(E, m_x) f_{\text{out}}(m_x) f_e \frac{I(m_x)}{4\pi L^2}$$

$$b(E, m_x) = b^{\delta}(m_x) \delta(E - m_x) + \\ + b^c(m_x) P_c(E, m_x)$$

$$P_c(E, m_x) = P\left(\frac{E}{m_x}\right) \sim \\ \sim \frac{1}{m_x} \left(\frac{E}{m_x}\right)^{-3/2} e^{-7.8 E/m_x}$$

From the new velocity, simple conservation of energy can determine the semi-major axis of the one-dimensional WIMP orbit:

$$\frac{1}{2}v_{surface}^2 - \frac{GM_{Sun}}{R_{Sun}} = 0 - \frac{GM_{Sun}}{a} \quad (4)$$

$$a = \left[\frac{1}{R_{Sun}} - \frac{v_{surface}^2}{2GM_{Sun}} \right]^{-1} \quad (5)$$

where a is the semi-major axis of the new WIMP orbit. From this and Kepler's laws, the orbital period is easily calculated:

$$Period = \frac{2\pi a^{3/2}}{G^{1/2}M_{Sun}^{1/2}} \quad (6)$$

After a number of orbits determined by the probability for a passing WIMP to interact with the Sun, the WIMP will further lose energy and a new semi-major axis and period will be calculated. This is continued until the new semi-major axis is less than the solar radius and total solar capture occurs. The total distance and total time spent outside of the Sun by the WIMP are calculated by summing the semi-major axes and periods including a factor reflecting the fraction of the orbit spent outside the Sun which is generally close to one.

The probability of a WIMP annihilating with another near-solar WIMP is calculated by integrating the product of the total distance traveled outside of the Sun prior to total solar capture, the WIMP-WIMP cross section and the number of density of WIMPs in the region. The WIMP-WIMP cross section can be approximated reasonably well and is generally on the order of $10^{-35}cm^2$ for a WIMP with velocity of a few hundred kilometers per second.⁴ The number density of near solar WIMPs is calculated by iteration in the monte carlo. It is approximated by a flat distribution extending to the mean semi-major axis of a near-solar WIMP orbit (usually around 2 solar radii). To determine if this approximation was valid, a distribution was calculated. It revealed a strong suppression at large distance from the Sun. The majority of WIMP interactions should occur within a few solar radii. The density distribution was normalized by the solar WIMP capture rate which is generally around 10^{21} WIMPs per second and varies inversely with WIMP mass.⁸

III. Results and Discussion

To begin calculating prospective event rates from near-solar WIMP annihilations, some assumptions are needed. The WIMP-WIMP and WIMP-proton cross sections are approximated by the standard weak coupling with appropriate suppressions. A value of $6 \times 10^{-42}cm^2$ was used for WIMP-proton interactions and a range of values from 2×10^{-36} to $2 \times 10^{-34}cm^2$ were used for WIMP-WIMP interactions. Three values of the WIMP mass were considered: 100, 300

Background

$$dN(x,t) = G(x) R(t) dx dt - \text{direct integration}$$

$$N_0 = \int [1 - \psi(x,t)] G(x) R(t) dx dt \quad \psi = \begin{cases} 0 & x \in \Omega(t) \\ 1 & x \notin \Omega(t) \end{cases}$$

$$dN_{\text{out}}(x,t) = \psi(x,t) G(x) R(t) dx dt$$

x - local coordinate

$$\psi = \begin{cases} 0, & x \in \bar{\Omega} \\ 1, & x \notin \bar{\Omega} \end{cases}$$

$$\Omega(t) \subset \bar{\Omega} \quad \forall t$$

$$\left\{ \begin{aligned} N_{\text{out}}(x) &= G(x) \int \psi(x,t') R(t') dt' \\ R_{\text{out}}(t) &= R(t) \int \psi(x',t) G(x') dx' \end{aligned} \right.$$

$$d(x) = \frac{N_0(x)}{N_{\text{out}}(x)} = \frac{\int [1 - \psi(x,t)] R(t) dt}{\int \psi(x,t) R(t) dt}$$

Li Ma statistic:

$$\bar{U} = \frac{\sum_x N_S(x) - \sum_x N_0(x)}{\sqrt{\sum_x d(x) N_S(x) + \sum_x N_0(x)}} =$$

$$= \frac{N_S - N_0}{\sqrt{\sum_x d(x) N_S(x) + N_0}}$$

$N_{hit} > 20$
 $N_{hit} > 60$
 $X_2 > 2.5$

Solar day only

Moon

Sun

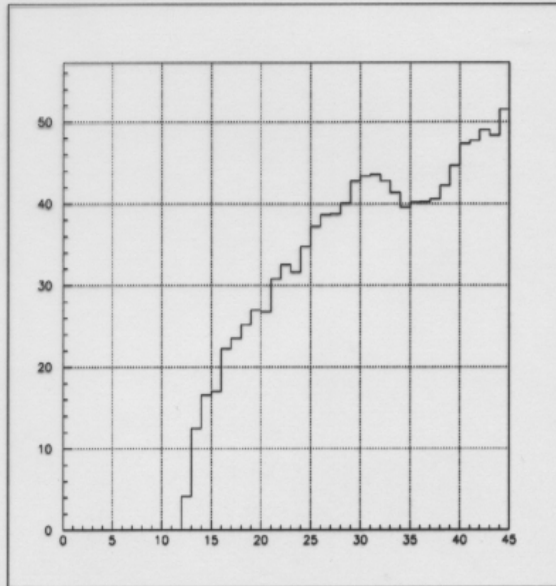
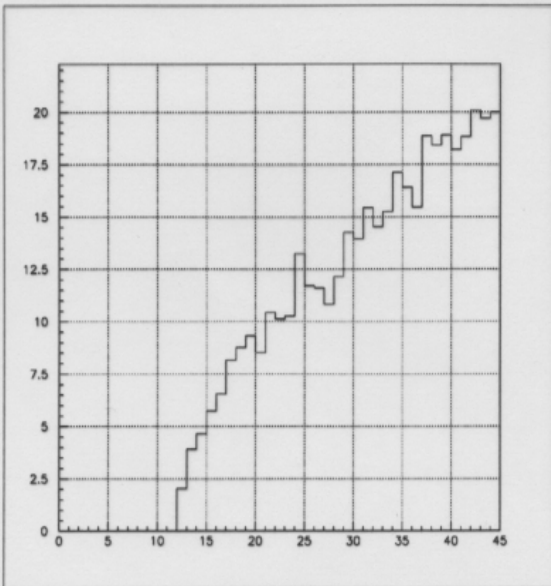
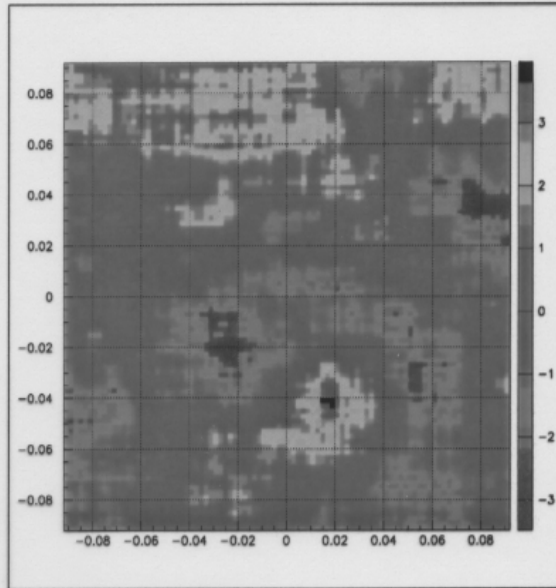
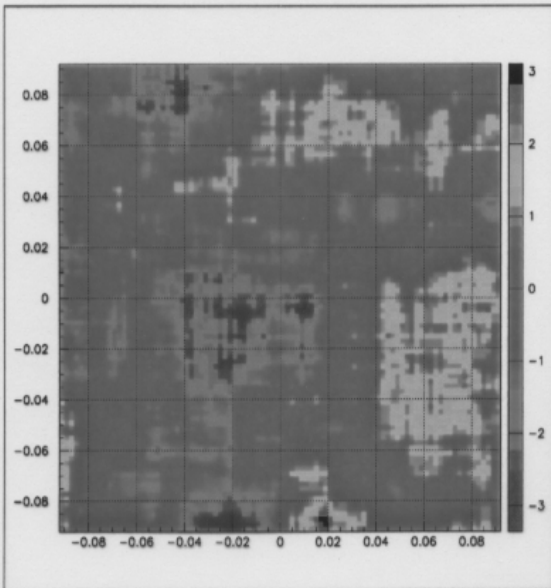


Figure 6.1: Significance maps of the regions of the sky around the daytime Moon(left) and the Sun(right) and the corresponding source exposure as function of zenith angle in hours per degree. The color code is in units of sigmas.

Flux limit

$$F_{\delta} \cdot \Delta + F_c \cdot \Sigma < 4791 \text{ events}$$

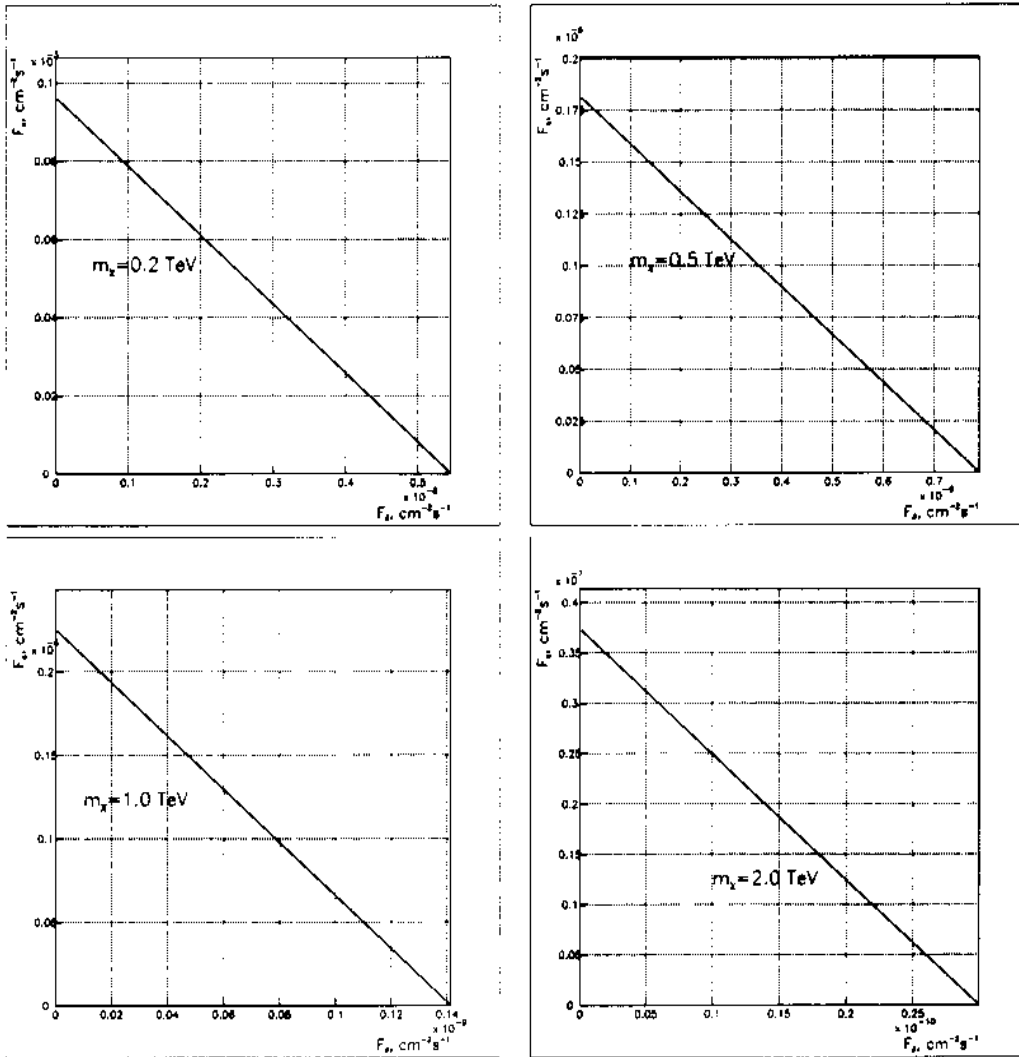


Figure 6: The values of (F_{δ}, F_c) below the line are allowed based the constructed upper limit.

$$\frac{dF}{dE} = F_{\delta} \cdot \delta(E - m_{\nu}) + \frac{F_c \left(\frac{E}{m_{\nu}} > 0.01 \right)}{m_{\nu}} \cdot \frac{\left(\frac{E}{m_{\nu}} \right)^{-3/2} e^{-7.8 E/m_{\nu}}}{\int_{0.01}^1 x^{-3/2} e^{-7.8 x} dx}$$

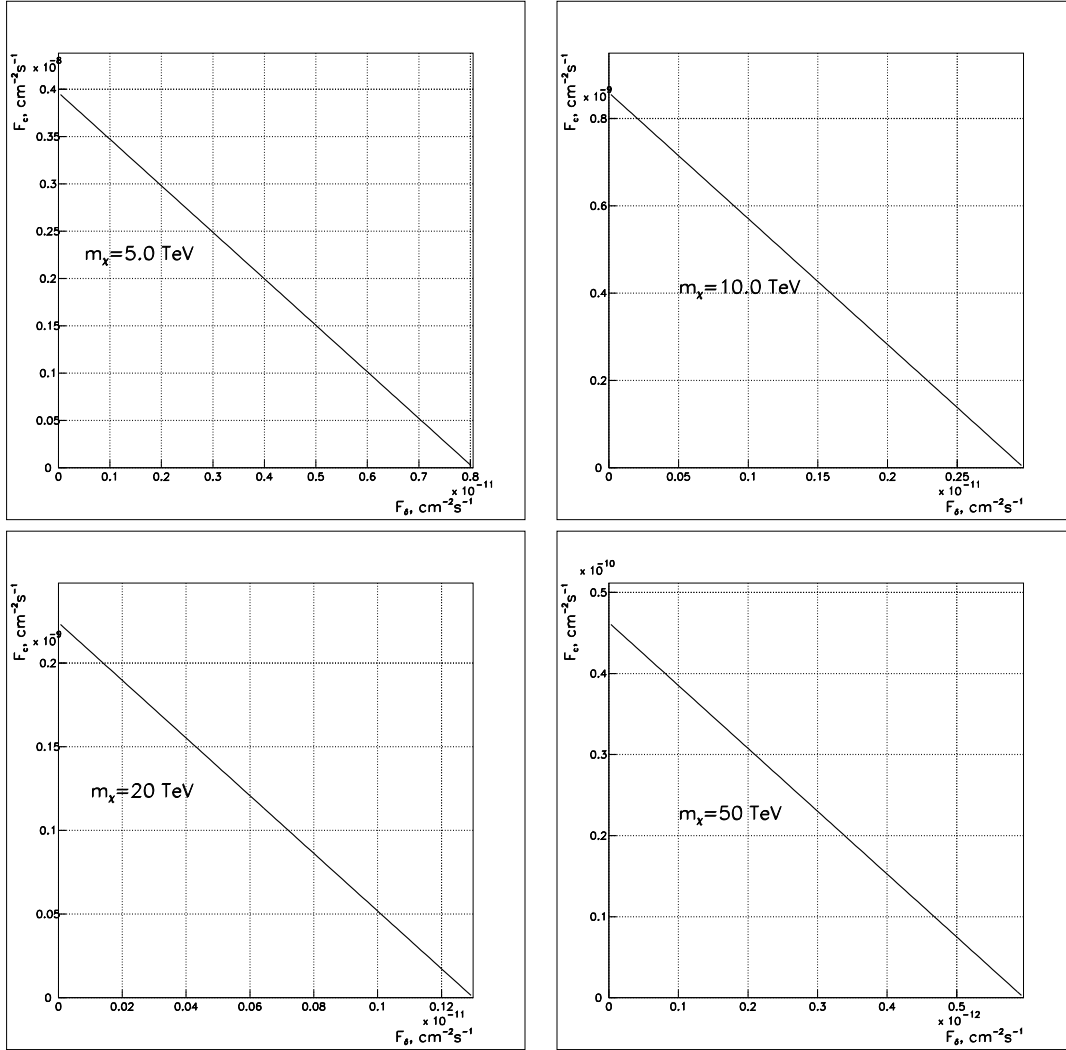


Figure 7: The values of (F_δ, F_c) below the line are allowed based the constructed upper limit.

	N_{on}	N_{on}^b	U
Sun	137211	137728	-1.35
Moon	49762	50064	-1.31

Table 1: Number of events in the optimal bin centered on the Sun and the Moon.

m_χ (TeV)	Δ (cm^2s)	Σ (cm^2s)
0.1	$1.055 \cdot 10^{11}$	0.000
0.2	$8.772 \cdot 10^{11}$	$4.969 \cdot 10^7$
0.5	$6.070 \cdot 10^{12}$	$2.634 \cdot 10^9$
1.0	$3.389 \cdot 10^{13}$	$2.127 \cdot 10^{10}$
2.0	$1.600 \cdot 10^{14}$	$1.280 \cdot 10^{11}$
5.0	$5.942 \cdot 10^{14}$	$1.208 \cdot 10^{12}$
10.0	$1.608 \cdot 10^{15}$	$5.575 \cdot 10^{12}$
20.0	$3.684 \cdot 10^{15}$	$2.136 \cdot 10^{13}$
50.0	$8.030 \cdot 10^{15}$	$1.035 \cdot 10^{14}$

Table 2: Coefficients of the flux limit calculation.

m_χ (TeV)	$F_\delta < (cm^{-2}s^{-1})$	$\frac{\sigma_{p\chi}}{10^{-43}cm^2} \frac{\rho_0}{0.3GeV/cm^3} b_\gamma <$
0.1	$4.54 \cdot 10^{-8}$	770
0.2	$5.46 \cdot 10^{-9}$	351
0.5	$7.89 \cdot 10^{-10}$	328
1.0	$1.41 \cdot 10^{-10}$	234
2.0	$2.99 \cdot 10^{-11}$	204
5.0	$8.06 \cdot 10^{-12}$	339
10.0	$2.98 \cdot 10^{-12}$	512
20.0	$1.30 \cdot 10^{-12}$	
50.0	$5.97 \cdot 10^{-13}$	

Table 3: The upper limit on the monochromatic photon flux due to near-solar neutralino annihilations and corresponding upper limit on the $\sigma_{p\chi}\rho_0 b_\gamma$.

$ u_c $	ξ_c
1.0	$1.587 \cdot 10^{-1}$
2.0	$2.275 \cdot 10^{-2}$
3.0	$1.350 \cdot 10^{-3}$
3.5	$2.326 \cdot 10^{-4}$
4.0	$3.167 \cdot 10^{-5}$
4.5	$3.398 \cdot 10^{-6}$
5.0	$2.867 \cdot 10^{-7}$

Table 4.1: Significance ξ_c and corresponding critical value u_c .

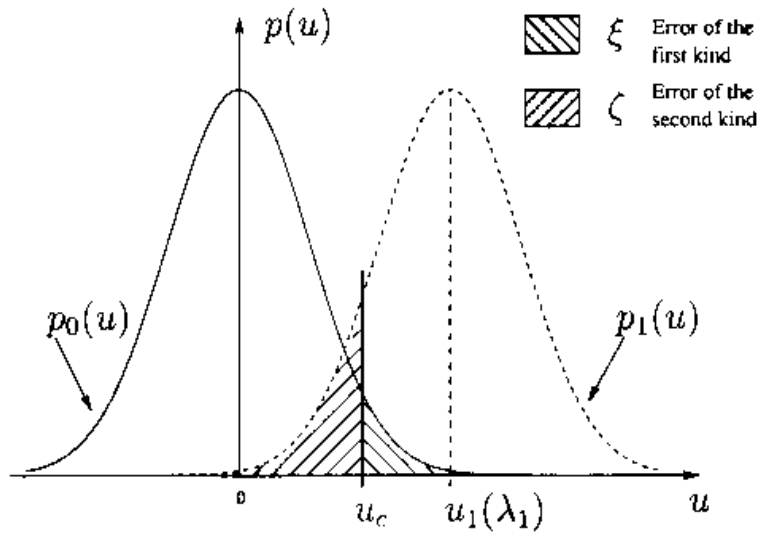


Figure 4.3: Critical region illustration for the statistic U when $\lambda_1 > \lambda$.

$$N \cdot \frac{u_c}{\sqrt{2}} < u_c \cdot \sqrt{2} \cdot \frac{u_c}{\sqrt{2}} = u_c \cdot \sqrt{2} \cdot \frac{u_c}{\sqrt{2}}$$

$$b^{\sigma} = 0.01 \quad \rho_0 = 0.3 \text{ GeV/cm}^3$$

$$\frac{1}{\lambda} = 2.9 \cdot 10^{-7} \quad \lambda = 3.4 \cdot 10^{-3}$$

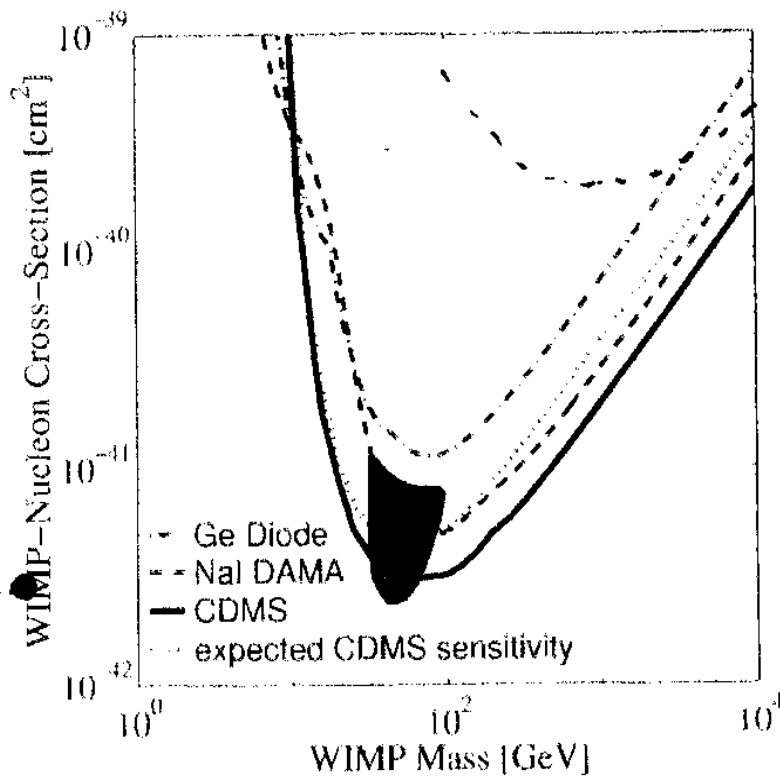


FIG. 4. Spin-independent σ vs M . The regions above the curves are excluded at 90% C.L. Solid curve: limit from this analysis. Dotted curve: CDMS expected sensitivity (median simulated limit) given the observed neutron background. Because the number of multiple scatters observed is larger than expected, the limit from this analysis is lower than the median simulated limit. Dashed curve: DAMA limit using pulse-shape analysis [31]. Shaded region: DAMA 3σ allowed region as described in text [28]. Dashed-dotted curve: Ge diode limit, dominated by [32,33]. All curves are normalized following [11], using the Helm spin-independent form factor, A^2 scaling, WIMP characteristic velocity $v_0 = 220 \text{ km s}^{-1}$, mean Earth velocity $v_E = 232 \text{ km s}^{-1}$, and $\rho = 0.3 \text{ GeV}/c^3 \text{ cm}^{-3}$.

Carlo simulation in order to determine the critical parame-

220 km s^{-1} it is determined. The data pre-allowed region. Furthermore, data and Fig. C.L. in the as support, non-compatible.

We thank surface event technical staff support. This Astrophysics operated by the operative Ag. Science. For by the D. No. DE-AC02 No. DE-FG02 by the Univ. Contract No. of Energy.

*Corresponding

Electronic

[1] V. Trubnikov

[2] P. J. E. P.

ton Univ.

[3] K. A. O.

(1998).

[4] B. W. Lee